Eur. Phys. J. A **17**, 223–234 (2003)
DOI 10.1140/epja/i2003-10006-6

THE EUROPEAN PHYSICAL JOURNAL A

Quark-hadron duality in electron-pion scattering

W. Melnitchouk[a]

Jefferson Lab, 12000 Jefferson Avenue, Newport News, VA 23606, USA

Received: 10 February 2003 /
Published online: 27 May 2003 –
Communicated by A. Schäfer

Abstract. We explore the relationship between exclusive and inclusive electromagnetic scattering from the pion, focusing on the transition region at intermediate Q^2. Combining Drell-Yan data on the leading twist quark distribution in the pion with a model for the resonance region at large x, we calculate QCD moments of the pion structure function over a range of Q^2, and quantify the role of higher twist corrections. Using a parameterization of the pion elastic form factor and phenomenological models for the $\pi \to \rho$ transition form factor, we further test the extent to which local duality may be valid for the pion.

PACS. 13.60.Hb Total and inclusive cross sections (including deep-inelastic processes) – 12.40.Nn Regge theory, duality, absorptive/optical models – 13.40.Gp Electromagnetic form factors

1 Introduction

The nature of the transition between quark and hadron degrees of freedom in QCD is one of the most fundamental problems in strong-interaction physics. This transition has been extensively explored within nonperturbative models of QCD, which, while retaining some of the apposite features of QCD, make simplifying assumptions that allow approximate solutions to be found [1]. Considerable progress has also been made recently in calculating hadronic properties directly from QCD via lattice gauge theory, and much is anticipated from this approach in the near future with significant advances in computing power available [2]. It is clear, however, that while a quantitative description of hadronic structure from first principles in QCD is still some time away, phenomenological input will remain crucial in guiding our understanding for the foreseeable future.

Of course, assuming QCD can ultimately describe the physics of hadrons, the transition from quarks and gluons to hadrons can be considered trivial in principle from the point of view of quark-hadron duality. So long as one has access to a complete set of states, it is immaterial whether one calculates physical quantities in terms of elementary quark or effective hadron degrees of freedom. In practice, however, truncations are unavoidable, and it is precisely the consequences of working with incomplete or truncated basis states that allows one to expose the interesting dynamics that drives the quark-hadron transition.

The duality between quarks and hadrons reveals itself in spectacular fashion through the phenomenon of Bloom-Gilman duality in inclusive lepton-nucleon scattering, $eN \to eX$. Here, the inclusive F_2 structure function of the nucleon measured in the region dominated by low-lying nucleon resonances is observed to follow a global scaling curve describing the high-energy data, to which the resonance structure function averages [3,4]. The equivalence of the averaged resonance and scaling structure functions in addition appears to hold for each prominent resonance region separately, suggesting that the resonance-scaling duality also exists, to some extent, locally.

The correspondence between exclusive and inclusive observables in electroproduction was studied even before the advent of QCD [5–10]. Within QCD, the appearance of duality for the moments of structure functions can be related through the operator product expansion (OPE) to the size of high twist corrections to the scaling structure function [11], which reflect the importance of long-range multi-parton correlations in the hadron [12]. The apparent early onset of Bloom-Gilman duality for the proton structure function seen in recent Jefferson Lab experiments [4] indicates the dominance of single-quark scattering to rather low momentum transfer [13]. It is not *a priori* clear, however, whether this is due to an overall suppression of coherent effects in inclusive scattering, or because of fortuitous cancellations of possibly large corrections. Indeed, there are some indications from models of QCD that the workings of duality may be rather different in the neutron than in the proton [14,15], or for spin-independent and spin-dependent structure functions.

From another direction, one knows from the large N_c limit of QCD [16] that duality is an inevitable consequence of quark confinement; in the mesonic sector one can prove

[a] e-mail: wmelnitc@jlab.org

(at least in 1+1 dimensions) that an exactly scaling structure function can be constructed from towers of infinitesimally narrow mesonic $q\bar{q}$ resonances [17]. This proof-of-principle example provides a heuristic guide to the appearance of the qualitative features of Bloom-Gilman duality, and has been used to motivate more elaborate studies of duality in quark models, even though application to the baryon sector is somewhat more involved [18]. Given that Bloom-Gilman duality is empirically established only for baryons (specifically, the proton), while the application of theoretical models is generally more straightforward in the meson sector, a natural question to consider is whether, and how, duality manifests itself phenomenologically for the simplest $q\bar{q}$ system in QCD —the pion.

As the lightest $q\bar{q}$ bound state, the pion plays a special role in QCD. Indeed, in Nature the pion presents itself as somewhat of a dichotomy: on the one hand, its anomalously small mass suggests that it should be identified with the pseudo-Goldstone mode of dynamical breaking of chiral symmetry in QCD; on the other, it ought to be described equally well from the QCD Lagrangian in terms of current quarks, with particularly attractive forces acting in the $J^P = 0^-$ channel. The complementarity of these pictures may also reflect, loosely speaking, a kind of duality between the effective, hadronic description based on symmetries, and a microscopic description in terms of partons. This duality is effectively exploited in calculations of hadron properties via the QCD sum rule method [19], in which results obtained in terms of hadronic variables using dispersion relations are matched with those of the OPE using free quarks.

In this paper we connect a number of these themes in an attempt to further develop and elucidate the issue of quark-hadron duality for the pion, focusing, in particular, on insights that can be gained from phenomenological constraints. Specifically, we shall examine the possible connections between the structure of the pion as revealed in exclusive scattering, and that which is measured in inclusive reactions. The latter can in principle be reconstructed given sufficient knowledge of the form factors which parameterize transitions from the ground-state pion to excited states. We do not attempt this rather challenging task directly; instead, we use the tools of the OPE to organize moments of the pion structure function according to (matrix elements of) local operators of a given twist. This exercise is possible because the structure function of the pion has been determined from Drell-Yan πN scattering data at high Q^2. Of course, the absence of fixed pion targets means that the structure of the pion at low excitation mass W is not known, with the exception of the elastic pion contribution, which has been accurately measured for $Q^2 \lesssim 2$ GeV^2 in π^+ electroproduction off the proton.

To complement the dearth of data on specific $\pi \to \pi^*$ transitions above threshold (but below the deep inelastic continuum), we consider a simple model for the pion structure function in which the low-W spectrum is dominated by the elastic and $\pi \to \rho$ transitions, on top of a continuum which is estimated by evolving the leading twist structure function to lower Q^2. The discussion at low W is necessarily more qualitative than for the corresponding case of the nucleon [20] where ample data exist. However, even within the current limitations, this analysis provides an estimate of the possible size of higher twist effects in the pion structure function, and the role of the resonance region in deep inelastic scattering (DIS) from the pion. Preliminary results for the higher twist corrections have been presented in ref. [21]. Here, we shall extend that analysis by considering the extent to which local duality may be valid in the pion structure function, and possible constraints on the $x \to 1$ behavior which can be inferred from the elastic channels.

This study is timely in view of experiments on the pion elastic [22,23] and transition [24,25] form factors being planned or analyzed at Jefferson Lab, which will probe the interplay between soft and hard scattering from the pion and the onset of perturbative QCD (pQCD) behavior. Furthermore, recent measurements of the inclusive pion structure function via the semi-inclusive charge-exchange reaction, $ep \to enX$, at HERA have yielded some unexpected results at low x [26], and new experiments over a large range of x are being planned at Jefferson Lab at lower Q^2 [27]. This paper discusses the possible interrelations between these measurements, in the quest for obtaining a consistent, unified description of the structure of the pion in electromagnetic scattering.

The structure of this paper is as follows. After briefly reviewing in sect. 2 the definitions and kinematics of inclusive lepton scattering from the pion, in sect. 3 we begin the discussion by focusing on the special case of elastic scattering. We construct an efficient parameterization of the elastic pion form factor in the space-like region consistent with the $Q^2 \to 0$ and $Q^2 \to \infty$ constraints. An analysis of moments of the pion structure function is presented in sect. 4, including the extraction of higher twists and a discussion of the role of the resonance region. Some of these results appeared in ref. [21]. In addition, we carefully examine the large-x region, which is important for high moments, and compare predictions of several models for the leading and higher twist contributions to the pion structure function as $x \to 1$. The relation of the structure function at $x \sim 1$ with the $Q^2 \to \infty$ dependence of elastic form factors is discussed in sect. 5, where we test the hypothesis of local Bloom-Gilman duality between the scaling structure function and the exclusive elastic and $\pi \to \rho$ transition contributions. Concluding remarks and a survey of future avenues for developments of the issues presented are outlined in sect. 6.

2 Definitions

Inclusive scattering of an electron, or any charged lepton, from a pion, $e\pi \to eX$, is described by the pion hadronic tensor,

$$W^{\pi}_{\mu\nu} = (2\pi)^3 \delta^4(p + q - p_X) \times \sum_X \langle \pi | J_\mu(0) | X \rangle \langle X | J_\nu(0) | \pi \rangle \ , \quad (1)$$

where p and q are the pion and virtual photon four-momenta, respectively, and p_X is the momentum of the hadronic final state with invariant mass squared $W^2 = m_\pi^2 - q^2 + 2m_\pi\nu$, with ν the energy transfer in the pion rest frame and m_π the pion mass. The hadronic tensor can be parameterized in terms of two structure functions,

$$W^\pi_{\mu\nu} = \left(-g_{\mu\nu} + \frac{q_\mu q_\nu}{q^2}\right) W_1^\pi(\nu, q^2) + \left(p_\mu - \frac{p\cdot q}{q^2} q_\mu\right)\left(p_\nu - \frac{p\cdot q}{q^2} q_\nu\right) \frac{W_2^\pi(\nu, q^2)}{m_\pi^2} , \quad (2)$$

where W_1^π and W_2^π are in general functions of two variables, for instance ν and q^2. In the limit as $\nu \to \infty$ and $Q^2 \equiv -q^2 \to \infty$, with $x = Q^2/2p\cdot q = Q^2/(W^2 - m_\pi^2 + Q^2)$ fixed, the functions W_1^π and νW_2^π become scale-invariant functions of x,

$$m_\pi W_1^\pi(\nu, q^2) \to F_1^\pi(x) , \quad (3a)$$

$$\nu W_2^\pi(\nu, q^2) \to F_2^\pi(x) . \quad (3b)$$

Furthermore, in this limit these functions satisfy the Callan-Gross relation, $F_2^\pi = 2xF_1^\pi$ [28]. Radiative QCD corrections introduce explicit dependence of $F_{1,2}^\pi$ on the strong-coupling constant, $\alpha_s(Q^2)$. While only transversely polarized photons contribute to the F_1^π structure function, $F_1^\pi \propto \sigma_T$, the F_2^π structure function receives both transverse and longitudinal contributions, $F_2^\pi \propto \sigma_T + \sigma_L$, where σ_T and σ_L are the transverse and longitudinal photoabsorption cross-sections, respectively.

3 Pion form factor

The inclusive spectrum begins with the elastic peak at $W = m_\pi$, or equivalently, $x = 1$. Because the pion is spinless, elastic scattering from the pion contributes only to the longitudinal cross-section, so that the elastic contribution to the F_1^π structure function vanishes. The elastic contribution to the F_2^π structure function is proportional to the square of the elastic pion form factor, $F_\pi(Q^2)$,

$$F_2^{\pi(\mathrm{el})}(x = 1, Q^2) = 2m_\pi\nu \left(F_\pi(Q^2)\right)^2 \delta(W^2 - m_\pi^2) , \quad (4)$$

where $F_\pi(Q^2)$ is the elastic pion form factor. As the most basic observable characterizing the composite nature of the lightest bound state in QCD, the elastic form factor of the pion is of fundamental importance to our understanding of hadronic structure. In the approximation that the pion wave function is dominated by its lowest $q\bar{q}$ Fock state, the pion form factor becomes amenable to rigorous QCD analysis. Indeed, it is well known that the asymptotic behavior of the pion form factor is calculable in pQCD [29–31],

$$F_\pi(Q^2) \to \frac{8\pi\alpha_s(Q^2)\, f_\pi^2}{Q^2} \quad \text{as} \quad Q^2 \to \infty , \quad (5)$$

where $f_\pi = 132$ MeV is the pion decay constant. Current data on F_π, summarized in fig. 1, indicate that there

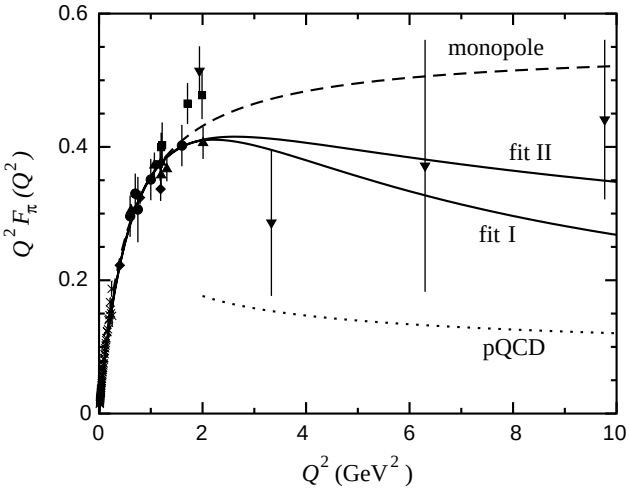

Fig. 1. Pion form factor as a function of Q^2. Shown are the best fits (solid lines) using eq. (6), a monopole fit (dashed line) with a cut-off mass of 0.74 GeV, and the asymptotic prediction from pQCD (dotted line).

are large soft contributions still at $Q^2 \lesssim 2$ GeV^2 [32,33]. The low-Q^2 data are obtained from scattering pions off atomic electrons [34], while the higher-Q^2 data are taken from ^{1}H$(e, e'\pi^+)n$ measurements at CEA/Cornell [35], DESY [36] and JLab [37]. For comparison, the leading-order pQCD prediction from eq. (5) is shown in fig. 1. Although the region of applicability of the pQCD result is *a priori* unknown, the pion represents the best hope of observing the onset of the asymptotic behavior experimentally (the corresponding pQCD calculation of the nucleon form factors significantly underestimates the data at the same Q^2).

There have been a number of calculations of the elastic pion form factor at low Q^2, for instance using the QCD sum rule approach [38]. Rather than rely on any specific model, however, in this analysis we use empirical data to calculate the elastic contribution to the pion structure function. For convenience, and for later use in sects. 4 and 5, we present a simple parameterization of the pion elastic form factor data in the space-like region, which is valid over the entire range of Q^2 currently accessible, and smoothly interpolates between the pQCD and photoproduction limits. For the latter, the pion form factor at low Q^2 can be well described in the vector meson dominance hypothesis, in which $F_\pi(Q^2) \sim 1/(1 + Q^2/m_\rho^2)$. A best fit to the low-$Q^2$ data using the simple monopole form is shown in fig. 1 (dashed line), with a cut-off mass ≈ 0.74 GeV. The monopole fit is not compatible, however, with the behavior at high Q^2 expected from pQCD. Building in the $Q^2 \to 0$ and $Q^2 \to \infty$ constraints, eq. (5), the available form factor data can be fitted by the form

$$F_\pi(Q^2) = \frac{1}{1 + Q^2/m_\rho^2}\left(\frac{1 + c_1 Z + c_2 Z^2}{1 + c_3 Z + c_4 Z^2 + c_5 Z^3}\right) , \quad (6)$$

where $Z = \log(1 + Q^2/\Lambda^2)$, and Λ is the QCD scale parameter. The form (6) is similar to that proposed in ref. [39]

Table 1. Fit parameters for the pion form factor in eq. (6), as discussed in the text.

	c_1	c_2	c_3	c_4
fit I	−0.201	0.020	−0.030	−0.093
fit II	0.100	0.060	0.538	−0.249

within a dispersion relation analysis; however, the form there uses 2 additional parameters, and takes a rather large value of $\Lambda \sim 1$ GeV. Note that the parameterization (6) is valid only in the space-like region; for a recent discussion of the properties of $F_\pi(Q^2)$ in the time-like region see ref. [40].

The best-fit parameters $c_{1...4}$ which give the minimum χ^2 are given in table 1. The parameter c_5 is constrained by the pQCD asymptotic limit, $c_5 = m_\rho^2(\beta_0/32\pi^2 f_\pi^2)c_2$, where $\beta_0 = 11-2N_f/3$ (= 9 for the 3-flavor case) [41]. For the QCD scale parameter we take $\Lambda = 0.25$ GeV. For completeness, we offer two parameterizations, which approach the pQCD limit (5) differently: in fit I the form factor becomes dominated by hard scattering at $Q^2 \sim 100$ GeV^2, consistent with semi-phenomenological expectations [33], while in fit II around half of the strength of the form factor at this scale still comes from soft contributions. These are indicated by the solid lines in fig. 1. Better quality data are needed to constrain $F_\pi(Q^2)$ at higher Q^2 ($\gtrsim 2$ GeV^2). To this end, there are plans to measure the pion form factor at an energy-upgraded Jefferson Lab to $Q^2 \approx 6$ GeV^2 [23].

4 Pion structure function

Going from elastic pion scattering ($W = m_\pi$) to the more general case of inelastic scattering ($W > m_\pi$), in this section we analyze the pion structure function, F_2^π, in terms of an OPE of its moments in QCD, and obtain an estimate for the size of higher twists corrections to the scaling contribution. Following this we discuss the role of higher twists in the pion structure function at large x, and compare several models for the $x \to 1$ behavior of F_2^π with data from Drell-Yan experiments.

4.1 Moments

From the operator product expansion in QCD, moments of the pion F_2^π structure function, defined as

$$M_n(Q^2) = \int_0^1 \mathrm{d}x\; x^{n-2}\; F_2^\pi(x, Q^2)\;, \qquad (7)$$

can be expanded perturbatively at large Q^2 as a power series in $1/Q^2$, with coefficients given by matrix elements of local operators of a given twist (defined as the mass dimension minus the spin of the operator),

$$M_n(Q^2) = \sum_{k=0}^{\infty} \mathcal{A}_k^n(\alpha_s(Q^2)) \left(\frac{1}{Q^2}\right)^k . \qquad (8)$$

Here the leading twist (twist 2) term $\mathcal{A}_0^n$ corresponds to free quark scattering and, modulo perturbative $\alpha_s(Q^2)$ corrections, is responsible for the scaling of the structure functions. The higher twist contributions $\mathcal{A}_{k>0}^n$ represent matrix elements of operators involving both quark and gluon fields, and are suppressed by additional powers of $1/Q^2$. The higher twist terms reflect the strength of non-perturbative QCD effects, such as multi-parton correlations, which are associated with confinement.

Note that the definition of $M_n(Q^2)$ includes the elastic contribution at $x = Q^2/(W^2 - m_\pi^2 + Q^2) = 1$, where W is the mass of the hadronic final state. Although negligible at high Q^2, the elastic contribution has been found to be important numerically at intermediate Q^2 for moments of the nucleon structure function [20]. In the definition (7) we use the Cornwall-Norton moments rather than the Nachtmann moments, which are expressed in terms of the Nachtmann scaling variable, $\xi = 2x/(1 + \sqrt{1 + 4x^2 m_\pi^2/Q^2})$, that includes effects of the target mass. The use of the Cornwall-Norton moments was advocated in ref. [20] on the grounds that it avoids the unphysical region $\xi > \xi(x = 1)$. Because of the small value of m_π, the difference between the variables x and ξ, and therefore between the x- and ξ-moments, is negligible for the pion.

The seminal analysis of De Rújula *et al.* [11] (see also ref. [20]) demonstrated that the onset of quark-hadron duality is governed directly by the size of the higher twist matrix elements. In particular, duality implies the existence of a region in the (n, Q^2) space in which the moments of the structure function are dominated by low-mass resonances, and where the higher twist contributions are neither dominant nor negligible. For the case of the proton F_2 structure function, even though there are large contributions from the resonance region, conventionally defined as $W \lesssim 2$ GeV, to the $n = 2$ moment ($\sim 70\%$ at $Q^2 = 1$ GeV^2), the higher twists contribute only around 10–20% to the cross-section at the same Q^2 [20]. The question we wish to address here is whether there exists an analogous region for the pion, where the resonance contributions are important, but higher twist effects are small enough for duality to be observed.

Of course, the distinction between the resonance region and the deep inelastic continuum is in practice somewhat arbitrary. In the large N_c limit of QCD, for instance, the final state in DIS from the pion is populated by infinitely narrow resonances even in the Bjorken limit, while the structure function calculated at the quark level produces a smooth, scaling function [14]. Empirically, the spectrum of the excited states of the pion is expected to be rather smooth sufficiently above the ρ mass, for $W \gtrsim 1$ GeV. Resonance excitation of heavier mesons is not expected to be easily discernible from the DIS continuum —the a_1-meson, for instance, at a mass $W \sim 1.3$ GeV, has a rather broad width ($\sim$ 350–500 MeV) [42].

Moments of the pion structure function can also be calculated directly via lattice QCD, and first simulations of the leading as well as some specific higher twist contributions have been performed [43]. Although the detailed

x dependence, especially at large x (see next section) requires knowledge of high moments [44], considerable information on the shape of the valence distribution can already be extracted from just the lowest 3 or 4 moments [45]. Calculations of a further 2 or 3 moments may be sufficient to allow both the valence and sea distributions to be extracted as a function of x.

Measurements of the pion structure function have been made using the Drell-Yan process [46–50] in πN scattering, covering a large range of x, $0.2 \lesssim x \lesssim 1$, and for Q^2 typically $\gtrsim 20$ GeV^2. It has also been extracted from the semi-inclusive DIS data at HERA for very low x and high W [26] (see also ref. [51]). However, there are no data on F_2^π at low W, in the region where mesonic resonances would dominate the cross-section. The spectrum could in principle be reconstructed by observing low-t neutrons produced in the semi-inclusive charge-exchange reaction, $ep \to enX$, where t is the momentum transfer squared between the proton and neutron, and extrapolating to the pion pole to ensure π exchange dominance. In the meantime, to obtain a quantitative estimate of the importance of the resonance region, we model the pion spectrum at low W in terms of the elastic and ρ pole contributions, on top of the DIS continuum evolved down from the higher-Q^2 region, as outlined in ref. [21]. The leading twist structure function can be reconstructed from parameterizations [52–54] of quark distributions in the pion obtained from global analyses of the pion Drell-Yan data. Unless otherwise stated, in this work we use the low-Q^2 fit from ref. [52], which gives the leading twist parton distributions in the pion for $Q^2 > 0.25$ GeV^2 (our conclusions are not sensitive to the use of other parameterizations [53,54]). For the elastic contribution we use the parameterization in eq. (6) (fit I).

The contribution of the ρ-meson is described by the $\pi \to \rho$ transition form factor, $F_{\pi\rho}(Q^2)$, which is normalized such that $F_{\pi\rho}(0) = 1$, and is expected to fall as $1/Q^4$ at large Q^2 (compared with $1/Q^2$ for $F_\pi(Q^2)$). Since there is no empirical information on $F_{\pi\rho}(Q^2)$, we consider several models in the literature, based on a relativistic Bethe-Salpeter vertex function [55], a covariant Dyson-Schwinger approach [56], and light-cone QCD sum rules [57]. These represent a sizable range ($\sim 100\%$) in the magnitude of $F_{\pi\rho}(Q^2)$ over the region of Q^2 covered in this analysis, with the calculation of ref. [57] giving a somewhat smaller result than those in refs. [55,56]. The spread in these predictions can be viewed as an indicator of the uncertainty in this contribution. The $\pi \to \rho$ transition form factor can be extracted, for instance, from ρ electroproduction data off the proton, $ep \to ep\rho^0$ [24,25], by reconstructing the decay of the ρ^0 into two pions. It also forms an important input into the calculation of meson-exchange current contributions to deuteron form factors at large Q^2 [58].

The contributions from the "resonance region", $W < W_{\rm res} \equiv 1$ GeV, to the moments of the pion structure function,

$$M_n^{\rm res}(Q^2) = \int_{x_{\rm res}}^1 {\rm d}x\; x^{n-2} F_2^\pi(x, Q^2) \;, \qquad (9)$$

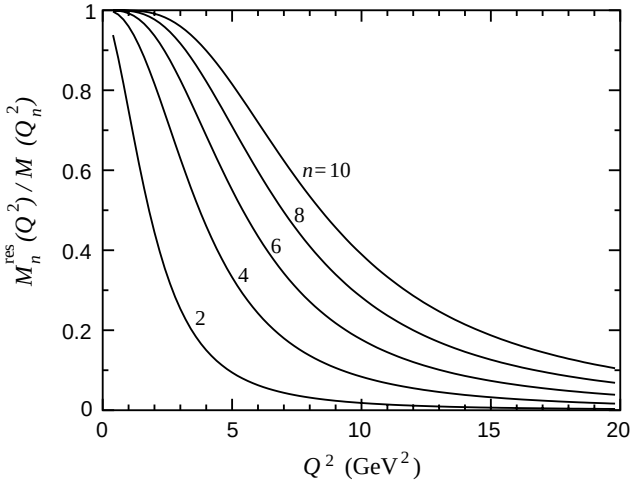

Fig. 2. Contributions to moments of the pion structure function from the resonance region, $W < W_{\rm res} = 1$ GeV, relative to the total.

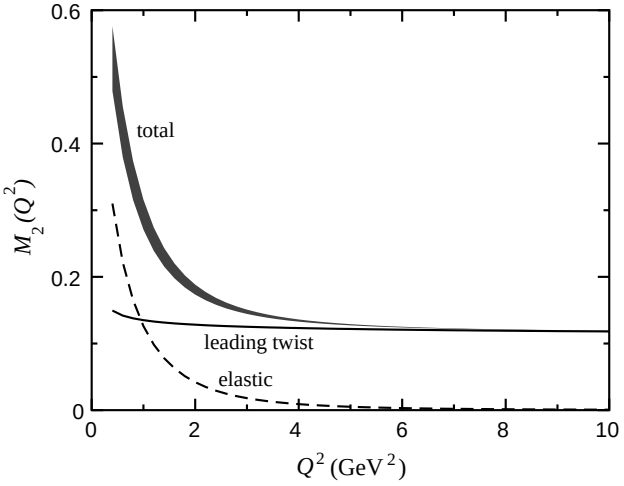

Fig. 3. Lowest ($n = 2$) moment of the pion structure function. The leading twist (solid line) and elastic (dashed line) contributions are shown, and the shaded region represents the total moment using different models for the $\pi \to \rho$ transition.

are plotted in fig. 2 as a ratio to the total moment, for $n = 2, \ldots, 10$. The integration in $M_n^{\rm res}(Q^2)$ is from $x_{\rm res} = Q^2/(W_{\rm res}^2 - m_\pi^2 + Q^2)$ to the elastic point, $x = 1$. The low-W region contributes as much as 50% at $Q^2 = 2$ GeV^2 to the total $n = 2$ moment, decreasing to $\lesssim 1\%$ for $Q^2 \gtrsim 10$ GeV^2 [21]. Higher moments are more sensitive to the large-x region, and subsequently receive larger contributions from low W. The $n = 10$ moment, for example, is almost completely saturated by the resonance region at $Q^2 = 2$ GeV^2, and even at $Q^2 = 10$ GeV^2 still receives some 40% of its strength from $W < 1$ GeV even at $Q^2 = 10$ GeV^2.

The relatively large magnitude of the resonance contributions suggests that higher twist effects play a more important role in the moments of the pion structure function than for the case of the nucleon. In fig. 3 the lowest

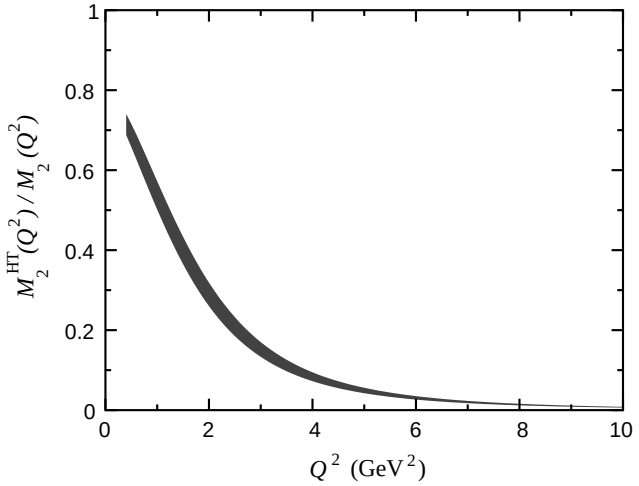

Fig. 4. Higher twist contribution to the $n = 2$ moment of the pion structure function, as a ratio to the total moment. The band indicates the uncertainty due to the model dependence of the $\pi \to \rho$ transition form factor.

$(n = 2)$ moment of F_2^π is displayed, together with its various contributions. The leading twist component,

$$M_n^{\rm LT}(Q^2) = \int_0^1 {\rm d}x\ x^{n-2} F_{2,{\rm LT}}^\pi(x, Q^2)\ , \qquad (10)$$

is expressed (at leading order in $\alpha_s(Q^2)$) in terms of the twist-2 quark distributions in the pion,

$$F_{2,{\rm LT}}^\pi(x, Q^2) = \sum_q e_q^2\ xq^\pi(x, Q^2)\ , \qquad (11)$$

where the valence part of q^π is normalized such that $\int {\rm d}x\ q_{\rm val}^\pi(x, Q^2) = 1$. The leading twist contribution is dominant at $Q^2 > 5$ GeV^2, while the deviation of the total moment from the leading twist at lower Q^2 indicates the increasingly important role played by higher twists there. While negligible beyond $Q^2 \approx 4$ GeV^2, the elastic contribution is as large as the leading twist already at $Q^2 \approx 1$ GeV^2. The $\pi \to \rho$ contribution is more uncertain, and the band in fig. 3 represents the total moment calculated using different models [55–57] of $F_{\pi\rho}(Q^2)$. However, while the current uncertainty in this contribution is conservatively taken to be $\sim 100\%$, doubling this would lead to a modest increase of the band in fig. 3. Uncertainty from poor knowledge of the leading twist distributions at small x [52–54] is not expected to be large.

To extract the higher twist part of the moments, one needs to subtract the leading twist contribution in eq. (10) from the total moments $M_n(Q^2)$,

$$M_n^{\rm HT}(Q^2) = M_n(Q^2) - M_n^{\rm LT}(Q^2) - M_n^{\rm TM}(Q^2)\ , \qquad (12)$$

where $M_n^{\rm TM}(Q^2)$ arises from target mass corrections. Because the target mass correction, which is formally of leading twist, is proportional to m_π^2/Q^2, its contribution will only be felt when $Q^2 \sim m_\pi^2$, which is far from the region where the twist expansion is expected to be valid. In principle nonperturbative effects can mix higher twist with higher-order effects in α_s, rendering the formal separation of the two problematic [59–62]. Indeed, the perturbative expansion itself may not even be convergent. However, by restricting the kinematics to the region of Q^2 in which the $1/Q^2$ term is significantly larger than the next-order correction in α_s, the ambiguity in defining the higher twist terms can be neglected [20]. In fig. 4 the higher twist contribution to the $n = 2$ moment is displayed as a function of Q^2. The band again represents an estimate of the uncertainty in the $\pi \to \rho$ transition form factor, as in fig. 3. At $Q^2 = 1$ GeV^2 the higher twist contribution is as large as the leading twist, decreasing to $\sim 1/3$ at $Q^2 = 2$ GeV^2, and vanishes rapidly for $Q^2 \gtrsim 5$ GeV^2.

As observed in ref. [21], the size of the higher twist contribution at $Q^2 \sim 1$ GeV^2 appears larger than that found in similar analyses of the proton F_2 [20] and g_1 [63] structure functions. This can be qualitatively understood in terms of the intrinsic transverse momentum of quarks in the hadron, $\langle k_T^2 \rangle$, which typically sets the scale of the higher twist effects. Since the transverse momentum is roughly given by the inverse size of the hadron, $\langle k_T^2 \rangle \sim 1/R^2$, the smaller confinement radius of the pion means that the average $\langle k_T^2 \rangle$ of quarks in the pion will be larger than that in the nucleon. Therefore, the magnitude of higher twists in F_2^π is expected to be somewhat larger ($\mathcal{O}(50\%)$) than in F_2^p. The E615 Collaboration indeed finds the value $\langle k_T^2 \rangle = 0.8 \pm 0.3$ GeV^2, within the higher twist model of ref. [64]. The experimental value is obtained by analyzing the $x \to 1$ dependence of the measured $\mu^+\mu^-$ pairs produced in πN collisions, and the angular distribution at large x. We discuss this in more detail below.

4.2 x → 1 behavior

The $x \to 1$ behavior of structure functions is important for several reasons. As discussed in the previous section, higher moments of F_2^π receive increasingly large contributions from the large-x region, so that a reliable extraction of higher twists from data requires an accurate determination of quark distributions at $x \sim 1$. In addition, since the $x \sim 1$ region is dominated by the lowest $q\bar{q}$ Fock state component of the pion light-cone wave function, in which the interacting quark carries most of the momentum of the pion, the behavior of the structure function at $x \to 1$ is expected to be correlated with that of the elastic form factor at $Q^2 \to \infty$. In this section we review various predictions for F_2^π in the limit as $x \to 1$, and relate these to the effects of higher twists discussed in the previous section on the $x \to 1$ behavior of the structure function.

Working within a field-theoretic parton model framework which predates QCD, Drell and Yan [5], and West [6] showed that if the asymptotic behavior of the form factor is $(1/Q^2)^n$, then the structure function should behave as $(1-x)^{2n-1}$ as $x \to 1$. This is referred to as the Drell-Yan-West (DYW) relation. Simple application to the case of the pion, in which the elastic form factor behaves as $1/Q^2$

at large Q^2, leads to the prediction

$$F_2^\pi(x \to 1) \sim (1-x) \ . \tag{13}$$

This behavior is also predicted in the model of ref. [8].

A dynamical basis for the exclusive-inclusive relation was provided with the advent of QCD. By observing that the interacting quark at large x is far off its mass shell, Farrar and Jackson [65] derived the $x \to 1$ behavior of the structure function at $x \to 1$ by considering perturbative one-gluon exchange between the q and $\bar{q}$ constituents in the lowest Fock state component of the pion wave function. They found a characteristic $\sim (1-x)^2$ dependence for the transverse part of F_2^π, in apparent contradiction with the naive DYW relation (the breakdown of the DYW relation for spinless hadrons was discussed earlier by Landshoff and Polkinghorne [9]). The longitudinal cross-section was found to scale like $1/Q^2$ relative to the transverse [65]. Using the so-called "softened" field theory [66], in which the pion-quark vertex function is described by a Bethe-Salpeter–type equation, Ezawa [10] found a similar $(1-x)^2$ behavior.

Gunion *et al.* [67] later generalized the gluon exchange description to include subleading $1/Q^2$ corrections for both the F_2^π and longitudinal F_L^π structure functions at $x \to 1$,

$$F_2^\pi(x) \sim S_2(1-x)^2 + \frac{T_2}{Q^2} \ , \tag{14}$$

$$F_L^\pi(x) \sim \frac{S_L}{Q^2} \ , \tag{15}$$

where the constants S_2, T_2 and S_L are determined phenomenologically. More generally, according to the pQCD "counting rules" [30], the leading components for any hadron with n spectator (noninteracting) partons were found [67] to behave as $(1-x)^{2n-1+2|\Delta S_z|}$ in the $x \to 1$ limit, where ΔS_z is the difference between the helicities of the hadron and the interacting quark. More recently, other nonperturbative models have been used to calculate the pion structure function [68]; however, because of difficulties associated with incorporating high-momentum components of the wave function, these may not be reliable in the $x \sim 1$ region.

The predicted $x \to 1$ behavior of the pion structure function can be tested by comparing with Drell-Yan data. The x dependence of the pion quark distributions has been measured in Drell-Yan $\mu^+\mu^-$ pair production in πN collisions (in practice, πA) at BNL [46], CERN [48,49] and at Fermilab [47,50]. The data for $q^\pi(x) \equiv u^{\pi^+}(x) = \bar{d}^{\pi^+}(x)$ from the most recent Fermilab experiment [50] are shown in fig. 5 for $4.05 < m_{\mu\mu} < 8.55$ GeV, where $m_{\mu\mu}$ is the invariant mass of the $\mu^+\mu^-$ pair. The scale dependence within this region was found to be small [50]. The data were fitted using the form

$$q^\pi(x, Q^2) = N x^a (1-x)^b + \gamma \ \frac{2\ x^2}{9\ Q^2} \ , \tag{16}$$

where N is a constant, fixed by normalization, and the scale Q^2 is identified with the the dimuon mass squared, $m^2_{\mu\mu}$. The form (16) parameterizes both leading and higher twist effects. Including corrections from Q^2 evolution, the best-fit value for the exponent governing the $x \to 1$ behavior was found to be $b \approx 1.21$–1.30 [50], consistent with the findings of the earlier CERN experiments [48,49]. The result of the leading twist E615 fit with $b = 1.27$ is shown in fig. 5 (dashed line). The forms $(1-x)$ [5,6,8] and $(1-x)^2$ [10,30,65,67,69] are also shown for comparison at large x (dotted lines). The data clearly favor a shape closer to $(1-x)$, rather than the $(1-x)^2$ shape implied by the counting rules [30].

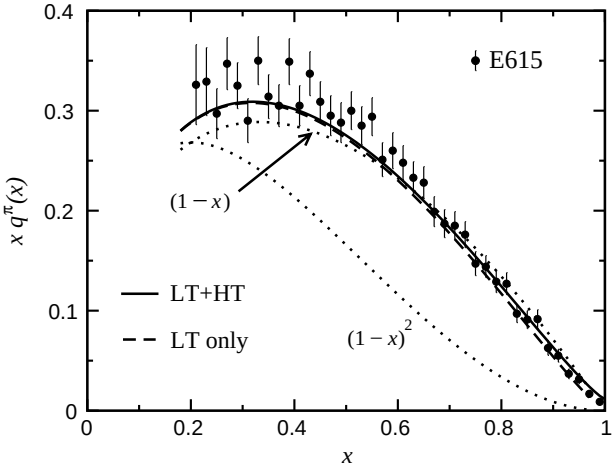

Fig. 5. Valence quark distribution in the pion extracted from the FNAL E615 Drell-Yan experiment [50], fitted with leading twist (dashed line) and leading + higher twist (solid line) contributions, as in eq. (16). The functional forms $(1-x)$ and $(1-x)^2$ (dotted lines) are shown for comparison.

It has been suggested [64] that higher twist effects in the pion structure function could obscure the true leading twist behavior. The higher twist coefficient T_2 was calculated in a pQCD-inspired model by Berger and Brodsky [64] in terms of the intrinsic quark momentum in the pion,

$$T_2 = \frac{2}{9} \frac{\langle k_T^2 \rangle}{Q^2} \ . \tag{17}$$

Since it is independent of x, it can be argued [64] that the higher twist contribution may in fact dominate the scaling term at fixed $Q^2(1-x)$ as $Q^2 \to \infty$, and mimic the observed $(1-x)$ dependence if $\langle k_T^2 \rangle \approx 1$ GeV^2. Conway *et al.* [50] subsequently performed an analysis of the E615 data by fitting also the term γ in eq. (16). The extracted value of b was found to be largely independent of the value of γ chosen. To investigate whether the quadratic term may be masked by an additional component not included in the model [64], Conway *et al.* searched for a nonzero intercept of F_2^π at $x = 1$. The fit with $\gamma = 0.83$ GeV^2 was found to be only marginally better than that with $\gamma = 0$ (the significance being 2.5 standard deviations), although the fit at $x \sim 1$ was also sensitive to the input nucleon sea distributions in the analysis of the Drell-Yan data. The leading + higher twist fit with $\gamma = 0.83$ GeV^2

is shown in fig. 5 (solid curve). The effect on the overall fit is indeed quite marginal, although at very large x ($\gtrsim 0.9$) the differences between this and the pure leading twist fit are more apparent.

Mueller [69] has pointed out that Sudakov effects, which introduce terms like $\alpha_s(Q^2)\ln^2(1/(1-x))$ into the $x \to 1$ analysis, may invalidate the usual renormalization group analysis of DIS at large x. Including power and double-logarithmic corrections, one finds that the $x \to 1$ behavior of F_2^π in this case becomes [69]

$$F_2^\pi \sim (1-x)^2 \exp\left\{-\frac{4C_F}{\beta_0}\left[\ln\frac{1}{1-x}\ln\ln Q^2 - \frac{\ln^2(1/(1-x))}{2\ln Q^2} - \ln\frac{1}{1-x}\ln\ln\frac{1}{1-x}\right]\right\} . \tag{18}$$

When $\ln(1/(1-x)) = \mathcal{O}(\ln Q^2/\ln\ln Q^2)$, higher twist terms compete with the leading twist, and the dominant contribution is then from the longitudinal structure function, which behaves as $F_L^\pi \sim (1/Q^2)\ln(Q^2(1-x))$. Taking this criterion literally, for $Q^2 \sim 1$ GeV^2 this would occur at $x \sim 0.93$, while for $Q^2 \sim 100$ GeV^2 the higher twists would be expected to dominate at $x \gtrsim 0.97$. A cautionary note regarding eq. (18), however, is that single-logarithmic effects have not been included in the analysis, and their effects on eq. (18) are unclear. Further discussion of these effects can be found in refs. [59,69]. Carlson and Mukhopadhyay [70] have also studied the effects of radiative corrections on the $x \to 1$ behavior of the structure function, and the appearance of higher twists in the low-W region. In particular, the scale dependence of the $(1-x)$ exponent was found to be $(1-x)^{b+c\ln\ln Q^2}$, with c calculable perturbatively. The Q^2-dependence of the pion structure function at $x \sim 1$ clearly deserves further study.

A cleaner signature of high twist effects at large x comes from the angular distribution of dimuon pairs produced in Drell-Yan collisions. The angular dependence of the Drell-Yan cross-section is given by [71] (see also ref. [72])

$$\frac{\mathrm{d}\sigma}{\mathrm{d}\Omega} \propto 1 + \lambda\cos^2\theta + \mu\sin 2\theta\cos\phi + \frac{\nu}{2}\sin^2\theta\cos 2\phi\,, \tag{19}$$

where the angles θ and ϕ are defined in the $\mu^+\mu^-$ rest system, and λ, μ and ν are functions of the kinematic variables. In the model of ref. [64], the leading twist $(1-x)^2$ term is associated with a $(1+\cos^2\theta)$ dependence, while the higher twist $\langle k_T^2\rangle/Q^2$ term has a characteristic $\sin^2\theta$ dependence. In particular, the transverse cross-section corresponds to $\lambda = 1$, while the deviation from a pure $(1+\cos^2\theta)$ dependence would indicate the presence of longitudinal or higher twist contributions. The data [50] are consistent with $\lambda = 1$ for $x \lesssim 0.6$, while the larger-x data show clear deviations from pure transverse scattering, suggesting the presence of higher twist contributions at these x values. With the fitted value of β (≈ 1.2–1.3), the measured x dependence of λ could be accommodated with $\langle k_T^2\rangle \approx 0.8$ GeV^2. Using the value $\beta = 2$ predicted by the pQCD counting rules, the observed λ values could be made to fit the data by requiring that $\langle k_T^2\rangle \sim 0.1$ GeV^2. However, in addition to being much smaller than the value $\langle k_T^2\rangle \sim 1$ GeV^2 suggested in ref. [64], this scenario is disfavored by a direct comparison with the x dependence of $q^\pi(x)$, as discussed above.

While the values of the quark intrinsic transverse momentum extracted from the Drell-Yan data are consistent with the size of the higher twist effects observed in sect. 3, there does appear to be a clear conflict between the counting rule predictions for the $x \to 1$ behavior of F_2^π and the empirical x dependence. Several reasons could account for this discrepancy. Even higher twist effects, beyond those of twist-4 parameterized in eq. (16), could be present and obfuscate an underlying $(1-x)^2$ leading twist behavior. This appears unlikely, however, given the relatively large Q^2 values ($Q^2 \gtrsim 20$ GeV^2) at which the data are sampled, and the rapid fall off of the higher twist contributions to the moments observed in sect. 4.1.

On the other hand, as alluded to above, the extraction of the pion structure function requires as input the parton distributions in the nucleon. Since the bulk of the data for $x > 0.5$ corresponds to a nucleon light-cone momentum fraction $x_N \approx 0.05$–0.1, errors may be introduced into the analysis through poor knowledge of the sea quark, or (at higher order) gluon, distributions in the nucleon. Furthermore, because the data are taken on nuclear targets (*e.g.* tungsten for the E615 experiment), nuclear effects may give rise to corrections to the nucleon quark distributions, especially in the region $x_N \sim 0.05$, where nuclear shadowing is known to play an important role [73]. The effects of using more modern nucleon parton distributions, and including nuclear corrections in the analysis, are currently being investigated [74].

It may also be that the asymptotic behavior does not set in until x is very close to 1, and that the functional form (16) is simply too restrictive to adequately reflect this behavior, in which case a more sophisticated parameterization would be required. Further, nonobservation of the predicted counting rule behavior may not necessarily imply a breakdown of pQCD. The derivation of the counting rules for large-x structure functions from Feynman diagrams in terms of hard gluon exchanges between quarks involves an infrared cut-off mass parameter, m, which regulates the integrals when $k_T \to 0$ [67,75]. Although an analysis based on pQCD should be valid also for $m = 0$, the counting rule results are sensitive to the parameter, m, and comparison with phenomenology requires a nonzero value [67].

Regardless of the ultimate $x \to 1$ behavior of F_2^π extracted from data, it is instructive to examine whether the asymptotic inclusive-exclusive relations between the pion structure function and the pion elastic and transition form factors at large Q^2 can provide additional constraints. In the next section we use local quark-hadron duality to study these relations in more detail.

5 Local quark-hadron duality

There has been a revival of interest recently in the phenomenon of Bloom-Gilman duality in electron-nucleon scattering. This has been stimulated largely by recent high-precision measurements [4] at Jefferson Lab of the F_2 structure function of the proton, which demonstrated that duality works remarkably well for each of the prominent low-lying resonance regions, including the elastic [76,77], as well as for the integrated structure function, to rather low values of Q^2. Ongoing and planned future studies will focus on duality in other structure functions, such as g_1 [78] and F_L [79], and for hadrons other than the proton.

While the existence of local quark-hadron duality appears inevitable in QCD at asymptotically large momenta [14,80], it is not *a priori* clear that it should work at finite Q^2. Indeed, there are reasons why at low Q^2 it should not work at all [14], and its appearance may in principle be due to accidental cancellations (due to quark charges in the proton [15,81], for instance) of possibly large higher twist effects. A systematic study of local duality for other hadrons, such as the pion, is therefore crucial to revealing the true origin of this phenomenon.

Shortly after the original observations of Bloom-Gilman duality for the proton [3], generalizations to the case of the pion were explored. By extending the finite-energy sum rules [82] devised for the proton duality studies, Moffat and Snell derived a local duality sum rule relating the elastic pion form factor with the scaling structure function of the pion [83],

$$[F_\pi(Q^2)]^2 \approx \int_1^{\omega_{\rm max}} {\rm d}\omega\ \nu W_2^\pi(\omega)\ , \qquad (20)$$

where $\nu W_2^\pi \equiv F_2^\pi$ is a function of the scaling variable $\omega = 1/x$. The upper limit $\omega_{\rm max} = 1 + (W^2_{\rm max} - m_\pi^2)/Q^2$ was set in ref. [83] by $W_{\rm max} \approx 1.3$ GeV, in order for the integration region to include most of the effect of the hadron pole, and not too much contribution from higher resonances [83]. To test the validity of the finite-energy sum rule relation (20), Moffat and Snell [83], and later Mahapatra [84], constructed Regge-based models of the pion structure function (their analyses predated the Drell-Yan pion structure function measurements [46–50]) to compare with the then available pion form factor data.

The existence of Drell-Yan data on F_2^π now allows one to test this relation quantitatively using *only* phenomenological input. Using parameterizations of the $F_2^\pi(x)$ data from ref. [50] (see fig. 5), the resulting form factor $F_\pi(Q^2)$ extracted from eq. (20) is shown in fig. 6. The agreement appears remarkably good. On the other hand, the magnitude of the form factor depends somewhat on the precise value chosen for $W_{\rm max}$, so the agreement in fig. 6 should not be taken too literally. Nevertheless, the shape of the form factor is determined by the x dependence of the structure function at large x. In particular, while a $(1-x)$ behavior leads to a similar Q^2-dependence to that for the E615 fit, assuming a $(1-x)^2$ behavior gives a form factor which drops more rapidly with Q^2. This simply reflects the kinematic constraint $(1 - 1/\omega) \sim 1/Q^2$ at fixed W.

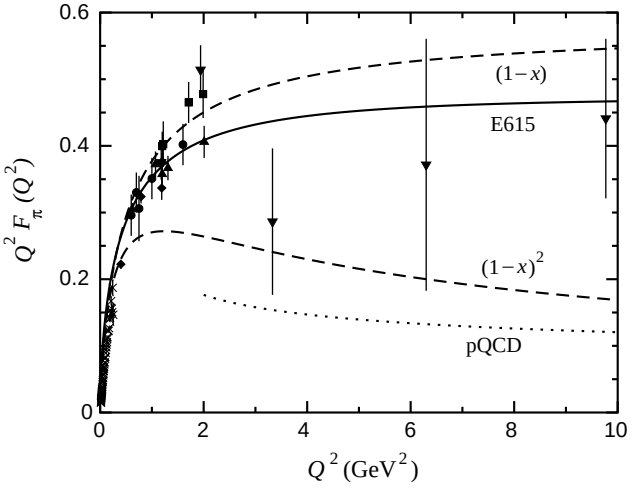

Fig. 6. Local duality prediction for the pion form factor, using phenomenological pion structure function input from the FNAL E615 Drell-Yan experiment [50] (solid line), and the forms $F_2^\pi(x) \sim (1-x)$ and $(1-x)^2$ (dashed lines). The asymptotic leading-order pQCD prediction (dotted line) is shown for reference.

Although the apparent phenomenological success of the local duality relation (20) is alluring, there are theoretical reasons why its foundations may be questioned. In fact, the workings of local duality for the pion are even more intriguing than for the nucleon. Because it has spin 0, elastic scattering from the pion contributes only to the longitudinal cross-section ($F_T^\pi(x = 1, Q^2) = 0$). On the other hand, the spin 1/2 nature of quarks guarantees that the deep inelastic structure function of the pion is dominated at large Q^2 by the transverse cross-section [11,65]. Taken at face value, the relation (20) would suggest a nontrivial duality relation between longitudinal and transverse cross-sections. Whether local duality holds individually for longitudinal and transverse cross-sections, or for their sum, is currently being investigated experimentally. Indications from proton data are that indeed some sort of duality holds for both the transverse and longitudinal structure functions of the proton individually [4,79].

While the elastic form factor of the pion is purely longitudinal, the $\pi \to \rho$ transition is purely transverse. It has been suggested [11] that the average of the pion elastic and $\pi \to \rho$ transition form factors may instead dual the deep-inelastic pion structure function at $x \sim 1$. If we take the simple model used in sect. 4 for the low-W part of the pion structure function, in which the inclusive pion spectrum at $W \lesssim 1$ GeV is dominated by the $\pi \to \pi$ and $\pi \to \rho$ transitions, we can estimate the degree to which such a duality may be valid. Generalizing eq. (20) to include the lowest-lying longitudinal and transverse contributions to the structure function, one can replace the left-hand side of (20) with $[F_\pi(Q^2)]^2 + \omega_\rho [F_{\pi\rho}(Q^2)]^2$, where $\omega_\rho = 1 + (m_\rho^2 - m_\pi^2)/Q^2$.

The sum of the lowest two "resonance" contributions (elastic + ρ) to the generalized finite-energy sum rule is shown in fig. 7 as a ratio to the corresponding leading twist DIS structure function over a similar range of W.

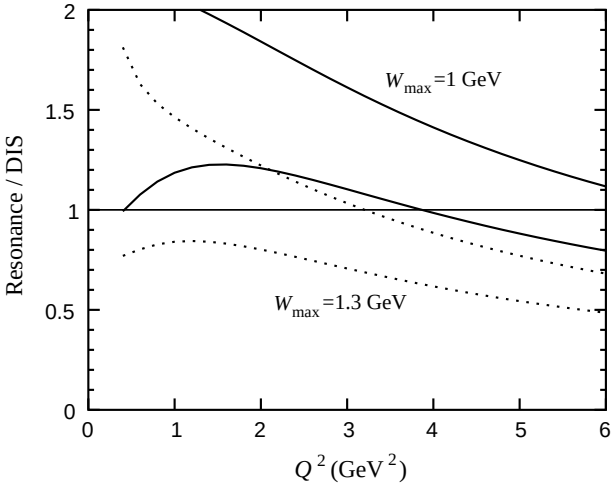

Fig. 7. Ratio of the pion resonance (elastic + $\pi \to \rho$ transition) contributions relative to the DIS continuum, for different values of $W_{\rm max}$. The two sets of upper and lower curves reflect the uncertainties in the $\pi \to \rho$ transition form factor.

The upper and lower sets of curves envelop different models [55–57] of $F_{\pi\rho}(Q^2)$, which can be seen as an indicator of the current uncertainty in the calculation. Integrating to $W_{\rm max} = 1$ GeV, the resonance/DIS ratio at $Q^2 \sim 2$ GeV^2 is $\sim 50 \pm 30\%$ above unity, and is consistent with unity for $Q^2 \sim$ 4–6 GeV^2 (solid curves). As a test of the sensitivity of the results to the value of $W_{\rm max}$, the resonance/DIS ratio is also shown for $W_{\rm max} = 1.3$ GeV (dotted curves). In this case the agreement is better for $Q^2 \sim$ 1–3 GeV^2, with the ratio being $\sim 30 \pm 20\%$ below unity for $Q^2 \sim$ 4–6 GeV^2.

Given the simple nature of the model used for the excitation spectrum, and the poor knowledge of the $\pi \to \rho$ transition form factor, as well as of the pion elastic form factor beyond $Q^2 \approx 2$ GeV^2, the comparison can only be viewed as qualitative. However, the agreement between the DIS and resonance contributions appears promising. Clearly, data on the inclusive π spectrum at low W would be invaluable for testing the local duality hypothesis more quantitatively. In addition, measurement of the individual transverse and longitudinal cross-sections of the pion, using Rosenbluth separation techniques, would allow duality to be tested separately for the longitudinal and transverse structure functions of the pion.

6 Conclusion

Understanding the structure of the pion represents a fundamental challenge in QCD. High-energy scattering experiments reveal its quark and gluon substructure, while at low energies its role as a Goldstone boson mode associated with chiral symmetry breaking in QCD is essential in describing the long-range structure and interactions of hadrons. We have sought to elucidate the structure of the pion by considering its response to electromagnetic probes, focusing in particular on the connection between inclusive and exclusive channels.

The relation between the pion structure function and the pion elastic and transition form factors has been studied in the context of quark-hadron duality. Moments of the pion structure function have been evaluated, and the role of the resonance region studied, assuming that the low-W resonant spectrum is dominated by the elastic and $\pi \to \rho$ transitions. The contribution of the resonance region ($W \lesssim 1$ GeV) to the lowest moment of F_2^π is $\sim 50\%$ at $Q^2 \approx 2$ GeV^2, and only falls below 10% for $Q^2 \gtrsim 5$ GeV^2. The elastic component, while negligible for $Q^2 \gtrsim 3$ GeV^2, is comparable to the leading twist contribution at $Q^2 \approx 1$ GeV^2. Combined, this means that the higher twist corrections to the $n = 2$ moment are $\sim 50\%$ at $Q^2 = 1$ GeV^2, $\sim 30\%$ at $Q^2 = 2$ GeV^2, and only become insignificant beyond $Q^2 \approx 6$ GeV^2.

Uncertainties on these estimates are mainly due to the poor knowledge of the inclusive pion spectrum at low W, which limits the extent to which duality in the pion can be tested quantitatively. Only the elastic form factor has been accurately measured to $Q^2 \approx 2$ GeV^2, although at larger Q^2 it is poorly constrained. The inclusive pion spectrum can be extracted from data from the semi-inclusive charge-exchange reaction, $ep \to enX$, at low t, for instance at Jefferson Lab [25]. This could also allow one to determine the individual exclusive channels at low W. In addition, a Rosenbluth separation would allow the transverse and longitudinal structure functions to be extracted.

Within the current uncertainties, the higher twist effects in the pion appear larger than the analogous corrections extracted from moments of the nucleon structure functions [20,63]. This can be generically understood in terms of the larger intrinsic transverse momentum of quarks, which governs the scale of the $1/Q^2$ corrections, in the pion than in the nucleon, associated with the smaller pion confinement radius. The implication is that duality would therefore be expected to set in later (at larger Q^2) for the pion than for the nucleon.

Higher twist effects have also been observed in the pion structure function at large x by the E615 Collaboration at Fermilab [50]. The x dependence and angular distribution of $\mu^+\mu^-$ pairs produced in πN collisions at $x \sim 1$ suggests a value $\langle k_T^2 \rangle = 0.8 \pm 0.3$ GeV^2, which is larger than the typical quark transverse momentum in the nucleon ($\mathcal{O}$(500 MeV)). On the other hand, the measured x dependence appears to be harder than that predicted by counting rules [30] or models based on perturbative one-gluon exchange [10,64,65,67], favoring a $(1-x)$ shape over a $(1-x)^2$ dependence. A reanalysis [74] of the Drell-Yan data to take into account nuclear corrections and updated sea quark distributions in the nucleon, which are used as input into the analysis, is necessary for a definitive assessment of the validity of the various approaches. Additional modification of the $x \to 1$ behavior due to Sudakov-like effects [69] may also need to be considered before drawing final conclusions about the implications of the observed $x \to 1$ dependence. There are also plans to measure F_2^π in semi-inclusive reactions over a range of x at Jefferson Lab [27] to confirm the Drell-Yan and semi-inclusive

HERA measurements, which should allow a more thorough exploration of the higher twist effects at lower Q^2.

The specific $x \to 1$ behavior of the pion structure function has consequences for the Q^2-dependence of the elastic pion form factor, if one assumes the validity of local quark-hadron duality for the pion. In particular, using parameterizations of the Drell-Yan structure function data, the existing data on $F_\pi(Q^2)$ can be fitted if the upper limit of the integration region above the elastic peak extends to $W_{\rm max} \approx 1.3$ GeV. Analogous fits with a $(1-x)^2$ shape fall off too rapidly with Q^2 and do not fit $F_\pi(Q^2)$ as well.

On the other hand, there may be limitations of the extent to which local duality can hold for the pion, as such duality implies a nontrivial relationship between the longitudinal and transverse cross-sections. It may in fact be more appropriate to examine whether the sum of the longitudinal (elastic) and transverse ($\pi \to \rho$ transition) contributions duals the DIS structure function at low W. Using phenomenological models for the $\pi \to \rho$ form factor, our estimate for the sum of the lowest-lying resonant contributions is in qualitative agreement with the corresponding scaling contribution in the same W interval. However, empirical information on the strength and Q^2-dependence of $F_{\pi\rho}(Q^2)$ is necessary for a more quantitative test. The $\pi \to \rho$ transition form factor can in practice be extracted from ρ electroproduction data [24]. At larger Q^2, the $\pi \to \rho$ transition is expected to be suppressed relative to the elastic contribution, and to test the local duality here will require a more accurate determination of $F_\pi(Q^2)$. The pion form factor $F_\pi(Q^2)$ will soon be measured to $Q^2 = 2.5$ GeV^2 at Jefferson Lab [22] in π^+ electroproduction from the proton, and possibly to $Q^2 = 6$ GeV^2 with an energy-upgraded facility [23].

Finally, this analysis can be easily extended to the strangeness sector, to study the duality between the form factor and structure function of the kaon. Data from the Drell-Yan reaction in K^--nucleus collisions [85] indicate that the quark distribution in the kaon is similar to that in the pion, and measurements of the kaon form factor, $F_K(Q^2)$, have also recently been reported [86]. Future measurements of $F_K(Q^2)$ at larger Q^2 (~ 2 GeV^2) [22] would allow the first quantitative test of local Bloom-Gilman duality in strange hadrons.

Helpful discussions with V. Burkert, R. Ent, P. Hoodbhoy, D. Mack, and K. Wijesooriya are gratefully acknowledged. I would also like to thank F. Gross, P. Maris and P. Tandy for sending the results of their form factor calculations. This work was supported by the U.S. Department of Energy contract DE-AC05-84ER40150, under which the Southeastern Universities Research Association (SURA) operates the Thomas Jefferson National Accelerator Facility (Jefferson Lab).

References

1. A.W. Thomas, W. Weise, *The Structure of the Nucleon* (Wiley-VCH, Berlin, 2001); R.K. Bhaduri, *Models of the Nucleon: from Quarks to Solitons* (Addison-Wesley, New York, 1988).
2. *Computational Infrastructure for Lattice Gauge Theory —A Strategic Plan* (April 2002), `www.lqcd.org/strategic-plan-04-04.pdf`.
3. E.D. Bloom, F.J. Gilman, Phys. Rev. Lett. **25**, 1140 (1970); Phys. Rev. D **4**, 2901 (1971).
4. I. Niculescu *et al.*, Phys. Rev. Lett. **85**, 1182; 1186 (2000).
5. S.D. Drell, T.-M. Yan, Phys. Rev. Lett. **24**, 181 (1970).
6. G.B. West, Phys. Rev. Lett. **24**, 1206 (1970); Phys. Rev. D **14**, 732 (1976).
7. J.D. Bjorken, J.B. Kogut, Phys. Rev. D **8**, 1341 (1973).
8. J.F. Gunion, S.J. Brodsky, R. Blankenbecler, Phys. Rev. D **8**, 287 (1973).
9. P.V. Landshoff, J.C. Polkinghorne, Nucl. Phys. B **53**, 473 (1973).
10. Z.F. Ezawa, Nuovo Cimento A **23**, 271 (1974).
11. A. De Rujula, H. Georgi, H.D. Politzer, Ann. Phys. (N.Y.) **103**, 315 (1977).
12. E. Stein, P. Gornicki, L. Mankiewicz, A. Schafer, Phys. Lett. B **353**, 107 (1995).
13. C.E. Carlson, N.C. Mukhopadhyay, Phys. Rev. D **41**, R2343 (1989); **47**, R1737 (1993); **58**, 094029 (1998).
14. N. Isgur, S. Jeschonnek, W. Melnitchouk, J.W. Van Orden, Phys. Rev. D **64**, 054005 (2001); S. Jeschonnek, J.W. Van Orden, Phys. Rev. D **65**, 094038 (2002).
15. F.E. Close, N. Isgur, Phys. Lett. B **509**, 81 (2001); F.E. Close, Q. Zhao, Phys. Rev. D **66**, 054001 (2002).
16. G. 't Hooft, Nucl. Phys. B **72**, 461 (1974); E. Witten, Nucl. Phys. B **160**, 57 (1979).
17. M.B. Einhorn, Phys. Rev. D **14**, 3451 (1976).
18. R. Dashen, A. Manohar, Phys. Lett. B **315**, 425; 438 (1993); R. Dashen, E. Jenkins, A. Manohar, Phys. Rev. D **49**, 4713 (1994).
19. M.A. Shifman, A.I. Vainshtein, V.I. Zakharov, Nucl. Phys. B **147**, 385, 448 (1979); A.I. Vainshtein, V.I. Zakharov, V.A. Novikov, M.A. Shifman, Sov. J. Nucl. Phys. **32**, 840 (1980).
20. X. Ji, P. Unrau, Phys. Rev. D **52**, 72 (1995).
21. W. Melnitchouk, JLAB-THY-03-01, Phys. Rev. D **67**, 077502 (2003).
22. H.P. Blok, G.M. Huber, D.J. Mack, nucl-ex/0208011; Jefferson Lab experiment E01-004.
23. L. Cardman *et al.* (Editors), *The Science Driving the 12 GeV Upgrade of CEBAF* (Jefferson Lab, 2001).
24. Jefferson Lab experiment E93-012, M. Kossov spokesperson.
25. V.D. Burkert, private communication.
26. G. Levman, J. Phys. G **28**, 1079 (2002).
27. Jefferson Lab proposal PR-01-110, R.J. Holt, P.E. Reimer, K. Wijesooriya spokespersons; and in *Hall a Preliminary Conceptual Design Report for the Jefferson Lab 12 GeV Upgrade* (2002).
28. C.G. Callan, D.J. Gross, Phys. Rev. Lett. **22**, 156 (1969).
29. G.R. Farrar, D.R. Jackson, Phys. Rev. Lett. **43**, 246 (1979).
30. G.P. Lepage, S.J. Brodsky, Phys. Rev. D **22**, 2157 (1980).
31. A. Duncan, A.H. Mueller, Phys. Rev. D **21**, 1636 (1980).
32. V.A. Nesterenko, A.V. Radyushkin, Phys. Lett. B **115**, 410 (1982).
33. N. Isgur, C.H. Llewellyn Smith, Phys. Rev. Lett. **52**, 1080 (1984).
34. S.R. Amendolia *et al.* Nucl. Phys. B **277**, 168 (1986).
35. C.J. Bebek *et al.*, Phys. Rev. D **17**, 1693 (1978).
36. P. Brauel *et al.*, Z. Phys. C **3**, 101 (1979).

37. J. Volmer *et al.*, Phys. Rev. Lett. **86**, 1713 (2001).
38. B.L. Ioffe, A.V. Smilga, Phys. Lett. B **114**, 353 (1982); Nucl. Phys. B **216**, 373 (1983).
39. K. Watanabe, H. Ishikawa, M. Nakagawa, hep-ph/0111168.
40. B.V. Geshkenbein, Phys. Rev. D **61**, 033009 (2000).
41. J.F. Donoghue, E.S. Na, Phys. Rev. D **56**, 7073 (1997).
42. D.E. Groom *et al.* (Particle Data Group), Eur. Phys. J. C **15**, 1 (2000).
43. C. Best *et al.*, Phys. Rev. D **56**, 2743 (1997); S. Capitani *et al.*, Nucl. Phys. B **570**, 393 (2000).
44. W. Detmold, W. Melnitchouk, A.W. Thomas, EPJ Direct C **13**, 1 (2001).
45. W. Detmold, W. Melnitchouk, A.W. Thomas, in preparation.
46. D. McCal *et al.*, Phys. Lett. B **85**, 432 (1979); J. Alspector *et al.*, Phys. Lett. B **81**, 397 (1979).
47. C.B. Newman *et al.*, Phys. Rev. Lett. **42**, 951 (1979).
48. J. Badier *et al.*, Z. Phys. C **18**, 281 (1983).
49. B. Betev *et al.*, Z. Phys. C **28**, 15 (1985).
50. J.S. Conway *et al.*, Phys. Rev. D **39**, 92 (1989).
51. M. Klasen, J. Phys. G **28**, 1091 (2002); B. Kopeliovich, B. Povh, I. Potashnikova, Z. Phys. C **73**, 125 (1996); H. Holtmann, G. Levman, N.N. Nikolaev, A. Szczurek, J. Speth, Phys. Lett. B **338**, 363 (1994); G.G. Arakelian, K.G. Boreskov, A.B. Kaidalov, Sov. J. Nucl. Phys. **33**, 247 (1981); J. Pumplin, Phys. Rev. D **8**, 2249 (1973); J.D. Sullivan, Phys. Rev. D **5**, 1732 (1972).
52. M. Gluck, E. Reya, A. Vogt, Z. Phys. C **53**, 651 (1992).
53. P.J. Sutton, A.D. Martin, R.G. Roberts, W.J. Stirling, Phys. Rev. D **45**, 2349 (1992).
54. M. Gluck, E. Reya, M. Stratmann, Eur. Phys. J. C **2**, 159 (1998).
55. H. Ito, F. Gross, Phys. Rev. Lett. **71**, 2555 (1993).
56. P. Maris, P.C. Tandy, Phys. Rev. C **65**, 045211 (2002).
57. A. Khodjamirian, Eur. Phys. J. C **6**, 477 (1999).
58. L.C. Alexa *et al.*, Phys. Rev. Lett. **82**, 1374 (1999).
59. A.H. Mueller, Phys. Lett. B **308**, 355 (1993).
60. E. Stein, M. Meyer-Hermann, L. Mankiewicz, A. Schafer, Phys. Lett. B **376**, 177 (1996).
61. S. Schaefer, A. Schafer, M. Stratmann, Phys. Lett. B **514**, 284 (2001).
62. S.I. Alekhin, A.L. Kataev, Phys. Lett. B **452**, 402 (1999); S.I. Alekhin, Phys. Rev. D **63**, 094022 (2001); hep-ph/0211096.
63. X. Ji, P. Unrau, Phys. Lett. B **333**, 228 (1994); X. Ji, W. Melnitchouk, Phys. Rev. D **56**, 1 (1997).
64. E.L. Berger, S.J. Brodsky, Phys. Rev. Lett. **42**, 940 (1979).
65. G.R. Farrar, D.R. Jackson, Phys. Rev. Lett. **35**, 1416 (1975).
66. S.J. Brodsky, G.R. Farrar, Phys. Rev. Lett. **31**, 1153 (1973).
67. J.F. Gunion, P. Nason, R. Blankenbecler, Phys. Rev. D **29**, 2491 (1984).
68. P. Castorina, A. Donnachie, Z. Phys. C **45**, 497 (1990); T. Shigetani, K. Suzuki, H. Toki, Phys. Lett. B **308**, 383 (1993); T. Frederico, G.A. Miller, Phys. Rev. D **50**, 210 (1994); R.M. Davidson, E. Ruiz Arriola, Phys. Lett. B **348**, 163 (1995); G. Altarelli, S. Petrarca, F. Rapuano, Phys. Lett. B **373**, 200 (1996); W. Bentz, T. Hama, T. Matsuki, K. Yazaki, Nucl. Phys. A **651**, 143 (1999); M.B. Hecht, C.D. Roberts, S.M. Schmidt, Phys. Rev. C **63**, 025213 (2001); F. Bissey *et al.*, hep-ph/0207107.
69. A.H. Mueller, Phys. Rep. **73**, 237 (1981).
70. C.E. Carlson, N.C. Mukhopadhyay, Phys. Rev. Lett. **74**, 1288 (1995).
71. C.S. Lam, W.K. Tung, Phys. Rev. D **18**, 2447 (1978); **21**, 2712 (1980).
72. A. Brandenburg, S.J. Brodsky, V.V. Khoze, D. Muller, Phys. Rev. Lett. **73**, 939 (1994).
73. W. Melnitchouk, A.W. Thomas, Phys. Lett. B **317**, 437 (1993); Phys. Rev. C **52**, 3373 (1995); G. Piller, W. Weise, Phys. Rep. **330**, 1 (2000).
74. K. Wijesooriya, private communication.
75. We thank P. Hoodbhoy for a discussion on this point.
76. R. Ent, C.E. Keppel, I. Niculescu, Phys. Rev. D **62**, 073008 (2000).
77. W. Melnitchouk, Phys. Rev. Lett. **86**, 35 (2001); Nucl. Phys. A **680**, 52 (2000).
78. V.D. Burkert, AIP Conf. Proc. **603**, 3 (2001), nucl-ex/0109004; T. Forest, in *Proceedings of the 9th International Conference on the Stucture of Baryons, Jefferson Lab, March 2002*; Jefferson Lab experiment E01-012, J.-P. Chen, S. Choi, N. Liyanage spokespersons; The HERMES Collaboration (A. Airapetian *et al.*), Phys. Rev. Lett. **90**, 092002 (2003).
79. M.E. Christy, in *Proceedings of the 9th International Conference on the Stucture of Baryons, Jefferson Lab, March 2002*; M.E. Christy, R. Ent, C. Keppel *et al.*, in preparation.
80. B.L. Ioffe, V.A. Khoze, L.N. Lipatov, *Hard Processes* (North-Holland, Amsterdam, 1984); B.L. Ioffe, JETP Lett. **58**, 876 (1993); S.A. Gurvitz, A.S. Rinat, Phys. Rev. C **47**, 2901 (1993); E. Pace, G. Salme, F.M. Lev, Phys. Rev. C **57**, 2655 (1998); L. Jenkovszky, V.K. Magas, E. Predazzi, Eur. Phys. J. A **12**, 361 (2001); R. Fiore, A. Flachi, L.L. Jenkovszky, A.I. Lengyel, V.K. Magas, hep-ph/0206027.
81. K. Gottfried, Phys. Rev. Lett. **18**, 1174 (1967).
82. R. Dolen, D. Horn, C. Schmid, Phys. Rev. **166**, 1768 (1968).
83. J.W. Moffat, V.G. Snell, Phys. Rev. D **4**, 1452 (1971).
84. B.P. Mahapatra, Phys. Lett. B **79**, 131 (1978).
85. J. Badier *et al.*, Phys. Lett. B **93**, 354 (1980).
86. O.K. Baker, Nucl. Phys. A **623**, 351C (1997).